

# A Theoretical and Experimental Study for Screening Inhibitors for Styrene Polymerization

## Authors:

Ali Darvishi, Mohammad Reza Rahimpour, Sona Raeissi

Date Submitted: 2019-12-09

Keywords: polymerization, styrene, stable nitroxide radicals, phenolic, inhibitors, density functional theory

## Abstract:

Styrene is one of the most important monomers utilized in the synthesis of various polymers. Nevertheless, during distillation, storage, and transportation of ST, undesired polymer (i.e., UP) formation can take place. Thus, the control of undesired polymerization of styrene is a challenging issue facing industry. To tackle the mentioned issue, the antipolymer and antioxidant activity of stable nitroxide radicals (i.e., SNRs) and phenolics in styrene polymerization were studied by density functional theory (DFT) calculation and experimental approach. The electrophilicity index and growth percentage have been determined by DFT calculation and experimental approach, respectively. It is depicted that 2,6-di-tert-butyl-4-methoxyphenol (DTMBP) and 2,6-di-tert-butyl-4-methylphenol (BHT) from phenolics, and 4-hydroxy-2,2,6,6-tetramethyl piperidine 1-Oxyl (4-hydroxy-TEMPO) and 4-oxo-2,2,6,6-tetramethylpiperidine 1-Oxyl (4-oxo-TEMPO) from stable nitroxide radicals were the most effective inhibitors. Also, the growth percentage of DTMBP, BHT, 4-hydroxy-TEMPO, and 4-oxo-TEMPO after 4 h were 16.40, 42.50, 24.85, and 46.8, respectively. In addition, the conversion percentage of DTMBP, BHT, 4-hydroxy-TEMPO, and 4-oxo-TEMPO after 4 h were obtained to be 0.048, 0.111, 0.065, and 0.134, respectively. Furthermore, the synergistic effect of these inhibitors was investigated experimentally, indicating that DTMBP/4-hydroxy-TEMPO exerted the best synergistic effects on the inhibition of polymerization. The optimum inhibition effect was observed at the blend of 4-hydroxy-TEMPO (25 wt.%) and DTMBP (75 wt.%) corresponding to 6.8% polymer growth after 4 h.

Record Type: Published Article

Submitted To: LAPSE (Living Archive for Process Systems Engineering)

Citation (overall record, always the latest version):

LAPSE:2019.1269

Citation (this specific file, latest version):

LAPSE:2019.1269-1

Citation (this specific file, this version):

LAPSE:2019.1269-1v1

DOI of Published Version: <https://doi.org/10.3390/pr7100677>

License: Creative Commons Attribution 4.0 International (CC BY 4.0)

Article

# A Theoretical and Experimental Study for Screening Inhibitors for Styrene Polymerization

Ali Darvishi, Mohammad Reza Rahimpour \*  and Sona Raeissi

Chemical Engineering Department, Shiraz University, Shiraz 71345, Iran; ali.darvishi2008@yahoo.com (A.D.); raeissi@shirazu.ac.ir (S.R.)

\* Correspondence: rahimpor@shirazu.ac.ir

Received: 23 August 2019; Accepted: 23 September 2019; Published: 1 October 2019



**Abstract:** Styrene is one of the most important monomers utilized in the synthesis of various polymers. Nevertheless, during distillation, storage, and transportation of ST, undesired polymer (i.e., UP) formation can take place. Thus, the control of undesired polymerization of styrene is a challenging issue facing industry. To tackle the mentioned issue, the antipolymer and antioxidant activity of stable nitroxide radicals (i.e., SNRs) and phenolics in styrene polymerization were studied by density functional theory (DFT) calculation and experimental approach. The electrophilicity index and growth percentage have been determined by DFT calculation and experimental approach, respectively. It is depicted that 2,6-di-tert-butyl-4-methoxyphenol (DTMBP) and 2,6-di-tert-butyl-4-methylphenol (BHT) from phenolics, and 4-hydroxy-2,2,6,6-tetramethyl piperidine 1-Oxyl (4-hydroxy-TEMPO) and 4-oxo-2,2,6,6-tetramethylpiperidine 1-Oxyl (4-oxo-TEMPO) from stable nitroxide radicals were the most effective inhibitors. Also, the growth percentage of DTMBP, BHT, 4-hydroxy-TEMPO, and 4-oxo-TEMPO after 4 h were 16.40, 42.50, 24.85, and 46.8, respectively. In addition, the conversion percentage of DTMBP, BHT, 4-hydroxy-TEMPO, and 4-oxo-TEMPO after 4 h were obtained to be 0.048, 0.111, 0.065, and 0.134, respectively. Furthermore, the synergistic effect of these inhibitors was investigated experimentally, indicating that DTMBP/4-hydroxy-TEMPO exerted the best synergistic effects on the inhibition of polymerization. The optimum inhibition effect was observed at the blend of 4-hydroxy-TEMPO (25 wt.%) and DTMBP (75 wt.%) corresponding to 6.8% polymer growth after 4 h.

**Keywords:** density functional theory; inhibitors; phenolic; stable nitroxide radicals; styrene; polymerization

## 1. Introduction

Over decades, styrene (ST) monomer has been employed to manufacture important commercial commodities such as acrylonitrile butadiene styrene (ABS), and styrene butadiene rubber (SBR) [1–4]. However, during distillation, storage, and transportation of ST, undesired polymer (UP) formation or organic peroxides fouling can presumably occur in the processing equipment, which reduces the heat transfer rate and increases the required time of cleaning [5,6].

In this respect, the three major mechanisms contributing to thermal self-initiation polymerization of styrene are Mayo, Flory, as well as a mechanism that is initiated through the reaction of oxygen and styrene, which are depicted in Figure 1, and explained briefly in the following.

Firstly, Mayo mechanism involves a Diels–Alder dimerization between two styrene molecules, which is followed by molecule-assisted hemolysis of dimer with a styrene molecule to produce two benzylic radicals. The high reactivity of the produced radicals initiate polymerization provided that they are added to a monomer (see r7).

Secondly, according to Flory mechanism, the initiation of styrene polymerization is attributed to the formation of a biradical, which is followed by biradical propagation through the addition of monomers on both active centers (see r1).

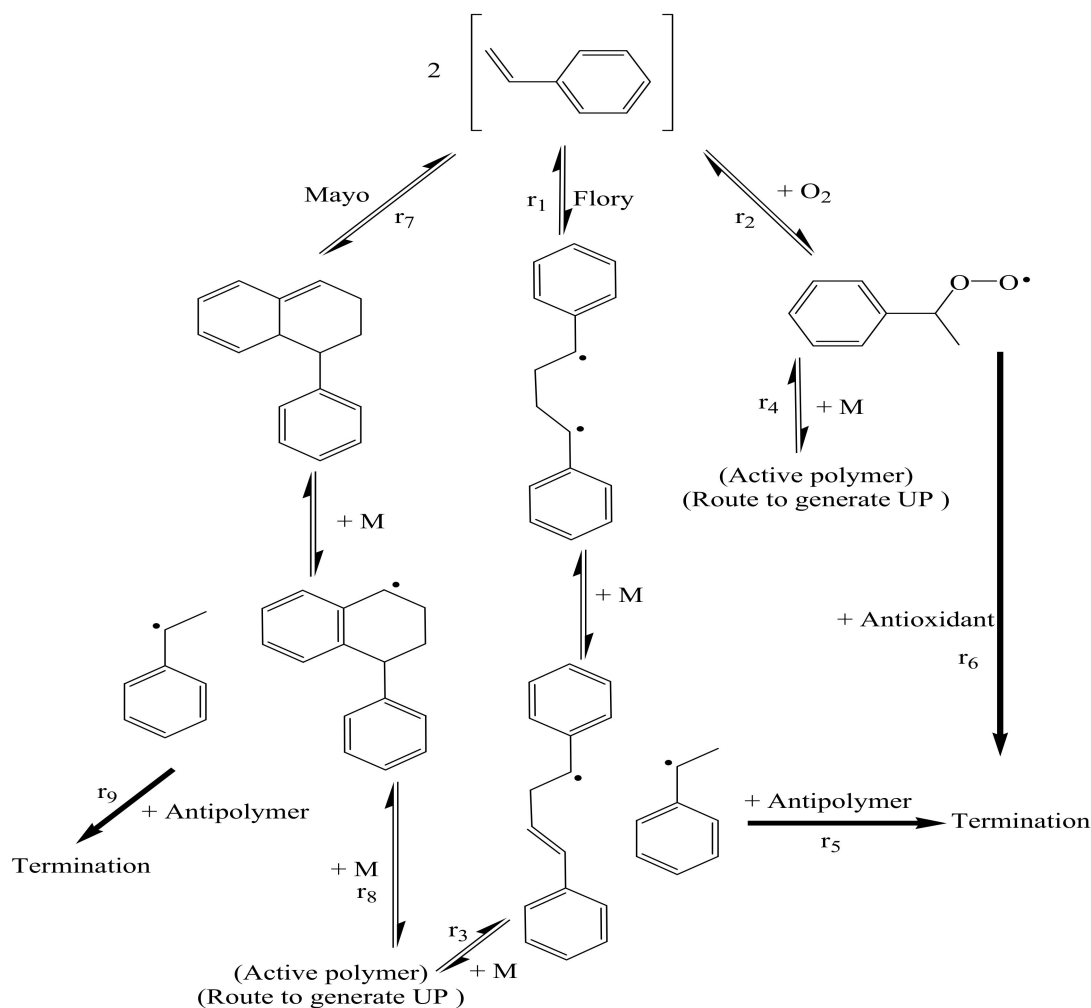


**Figure 1.** Reaction mechanism for styrene (ST) polymerization. Hydrogen atoms are omitted for clarity.

Thirdly, regarding the oxygen-related mechanism, the oxygen reacts with some of the ST molecules to form an organic peroxide (r2). Following that, considering the fact that organic peroxides are very reactive molecules containing very weak oxygen–oxygen single bonds that can break easily to give free radicals, chain-growth polymerization occurs. Then, these chain-extended polymers react with another monomer, further extending the polymer chains, and subsequently produce very stable compounds. As a result, these stable compounds tend to sediment easily as undesired polymers regarding their low activity in the reaction [7,8].

It should be noted that under some specific conditions, the UP formation can be intensified. By way of illustration, the autocatalytic phenomenon has been reported to take place in the styrene polymerization at high temperatures of around 85 to 130 °C [9–12].

Moreover, the number of methylene groups can play a key role in intensifying polymerization. Indeed, a polymer with greater number of methylene groups exhibit higher activity to react with oxygen, and consequently intensify UP formation.

Furthermore, exposure to heat and light have also been reported as other factors contributing to more severe UP formation. As a matter of fact, when ST monomer is exposed to heat or light, generation of free radicals (ST\*) is accelerated, which eventually results in more rapid polymerization. More details of free radical polymerization mechanism can be found elsewhere [13–18].

To talk about the configuration of the UP such as polystyrene, it is in fact highly dependent on the spatial structure of monomer and how it is added to the growing radical chain during polymerization. For example, the polymerized polystyrene formed undesirably is regarded as an atactic polymer; in other words, it has an amorphous' structure. The production of polystyrene through the radical polymerization leads to formation of atactic polymers in the polymer chains [19].

To address the mentioned issues regarding UP formation, a practical method for the removal of undesired polymers is the mechanical cleaning in which the disassembly of apparatus is inevitable. Nevertheless, this procedure is undeniably accompanied by some drawbacks. As a matter of fact, it is time-consuming, expensive, and also total elimination of UP cannot thoroughly be accomplished through the mechanical cleaning. As a result, the remaining UP could further intensify the growth of UP in the next operation cycles [5,6].

Accordingly, various inhibitors have been suggested to prevent undesired polymer formation [6,20]. Generally, according to mechanism of action, they could be classified into two main types of materials, i.e., acceptor type and donor type, which are called antipolymers and antioxidants, respectively, and are discussed briefly in the following [21].

In the first place, the acceptor radical inhibitors (i.e., antipolymers) are capable of oxidizing the alkyl radicals by accepting hydrogen or even an electron via an addition mechanism through reactions r5 and r9 in Figure 1. The recombination of radicals is an important termination route in any polymerization pathway. As the concentration of radicals increases, the rate of recombination increases as well. These antipolymers directly react with the radical to remove it from the propagation. Acceptor radical inhibitors are efficient in the low-oxygen environments for the deactivation of alkyl radicals [22]. It should be noted that these antipolymers are injected in low concentrations, indicating their low amount of consumption for the purpose of antipolymerization. These inhibitors have quite rapid action on propagator radicals. In fact, they can transform initiator and propagator radicals into either non-radical form or radicals with low reactivity in propagation reaction, and thus inhibiting the radical polymerization [23,24].

By way of illustration, stable nitroxide radicals (SNRs) are typical antipolymers, which are able to terminate the propagation chains through the reaction pathway demonstrating in Figure 2.

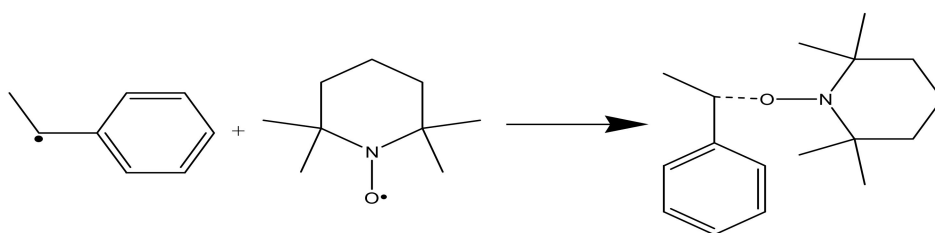


**Figure 2.** Mechanism of inhibition of styrene polymerization by a typical nitroxide radical. Hydrogen atoms are omitted for clarity.

In the second place, radical donor inhibitors (i.e., antioxidant), as shown in Figure 1, tend to reduce proxy radicals by giving a hydrogen or an electron (see reaction r6). As a result, in contrast with antipolymers, antioxidants exhibit more favorable performance in oxygen-rich environments. Actually, as mentioned before, oxygen can act as the initiator of the polymerization when attacks the styrene molecules. As a consequence, in the absence of antioxidant, ST monomer can react with peroxide radicals to form peroxide chains (see reaction r4), and subsequently lead to formation of UP. This is where the role of using antioxidants becomes noticeable as it can shift the reaction pathway from reaction 4 to reaction 6, which is followed by less polymer formation in the process.

It can generally be claimed that antioxidants are capable of suppressing the formation of new UP seeds. However, they cannot stop UP polymerization thoroughly. To compare the performance of antioxidant with antipolymers, the reaction rate of antioxidants is much lower than that of the

antipolymers. Accordingly, they are consumed more slowly, and hence their preventing effects last longer [22,25].

Possible pathways of inhibition in the presence of phenolic antioxidants are shown in Figure 3 [26,27]. The mechanisms of Figure 3a,b occur in the absence of oxygen, while the mechanism in Figure 3c, which is faster than the two former ones, occurs in the presence of oxygen [26–29]. The conventional representative of phenolic antioxidant is 4-tert-butylpyrocatechol (TBC) [5,6,27,30].

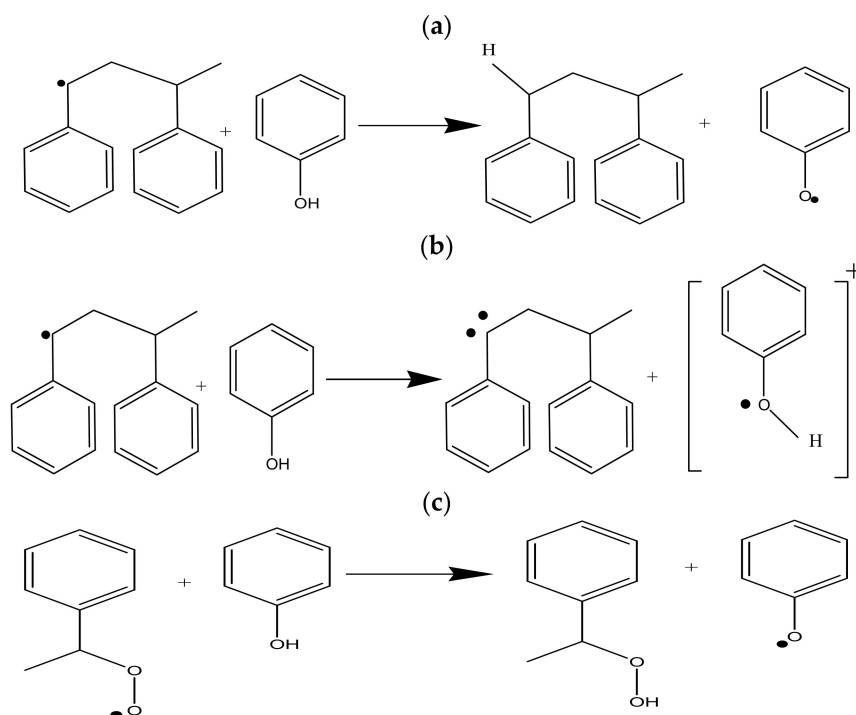


**Figure 3.** Mechanism of (a): H-atom donation, (b) electron donation, and (c) H-atom donation reaction in the presence of oxygen by typical phenolics. Hydrogen atoms are omitted for clarity.

Nonetheless, in almost all cases, both routes of r1-r3, r7-r8, and r2-r6 successive reactions occur simultaneously to generate UP. Therefore, the main drawback of utilizing antioxidants or antipolymers is that they are not individually capable of inhibiting both routes of UP formation. To address the mentioned issue, the utilization of antipolymer/antioxidant blends has been proposed as the state of the art currently [31–33]. This strategy would result in the simultaneous inhibition of three UP routes.

In order to study the mechanisms and performance of inhibition processes, the two major approaches are experimental evaluation and mathematical calculations such as density functional theory (DFT).

The DFT method demonstrates advantageous features including less demanding computational effort and computing time in conjunction with better agreement with experimental results relative to other procedures. (e.g., Hartree–Fock base method) [34,35]. In fact, the results of calculation through this method are in an acceptable agreement with the experimental chemical properties such as electron-withdrawing of some components. For instance, it is generally known that the reactivity of antioxidant and antipolymer is related to the electron withdrawing tendency of the moieties [36,37]. In addition, Pellecchia and Grassi [38] reported that electron-releasing substituent atom or group enhanced polymerization, whereas the electron-withdrawing substituent atom or group acted as deactivator. Thus, in order to evaluate the electron-withdrawing property of a component, DFT calculations can appropriately be applied.

The main objective of the present study is the investigation of approaches and remedies for eliminating, or at least reducing the blockage of styrene purification units occurred by undesired polymerization. In this regard, a combination of theoretical and experimental approaches is employed

to screen and compare different inhibitors including SNRs and phenolics. Furthermore, the synergic effect of antipolymer/antioxidant blends on the undesired ST polymerization is investigated. For the purpose of screening new inhibitors, DFT method is implemented, which can be conducted without experiment. The results of the present study would shed light on the impact of UP inhibitors and pave a reliable path to the optimum utilization of these inhibitors.

## 2. Method

### 2.1. Theoretical

In the present study, the global electrophilicity index is utilized as a criterion for the usefulness of different additives in polymerization inhibition. This index can be determined by employing DFT calculations. In fact, in order to calculate the electrophilicity index (i.e.,  $\omega$ ) two other parameters including  $\eta$  (i.e., chemical hardness of a radical) and  $\mu$  (i.e., global chemical potential) indexes are firstly required to be calculated (see Equations (1)–(3)) [39,40]. The  $\eta$  index is the degree of persistence to the charge transfer, while the  $\omega$  index is the degree of tendency of an atom to attract electrons. The  $\mu$  index demonstrates the stabilization energy of the components and their electron affinity. In order to calculate  $\mu$  and  $\eta$ , in the first place,  $E_{\text{LUMO}}$  and  $E_{\text{HOMO}}$  should be determined through DFT calculations (UB3LYP/6-311+G level).

$$\eta = (E_{\text{LUMO}} - E_{\text{HOMO}})/2 \quad (1)$$

$$\mu = (E_{\text{HOMO}} + E_{\text{LUMO}})/2 \quad (2)$$

$$\omega = \mu^2/2\eta \quad (3)$$

where  $E_{\text{LUMO}}$  denotes electron energies of the lowest unoccupied molecular orbital (i.e., LUMO) and  $E_{\text{HOMO}}$  indicates electron energies of the highest occupied molecular orbital for a neutral component (i.e., HOMO). Higher HOMO energy corresponds to stronger electron-donating ability of the molecule [41–46].

### 2.2. Experimental

#### 2.2.1. Material

2,2,6,6-tetramethylpiperidine 1-Oxyl (TEMPO, 98%), 4-Amino-2,2,6,6-tetramethylpiperidine 1-Oxyl (4-amino-TEMPO, 97%), 4-hydroxy-2,2,6,6-tetramethylpiperidine 1-Oxyl (4-hydroxy-TEMPO, 97%), 4-oxo-2,2,6,6-tetramethylpiperidine 1-Oxyl (4-oxo-TEMPO, 97%), 2,6-di-tert-butyl-4-methylphenol (BHT, 99%), Tert-butyl hydroquinone (TBHQ, 97%), 2,6-di-tert-butyl-4-methoxyphenol (DTBMP, 98%), and 4-Methoxyphenol (MEHQ, 98%) were supplied from Sigma Aldrich. The structures of inhibitors sketched by DFT are summarized in Figure 4. Styrene, styrene polymer, and TBC were supplied from the domestic plant.

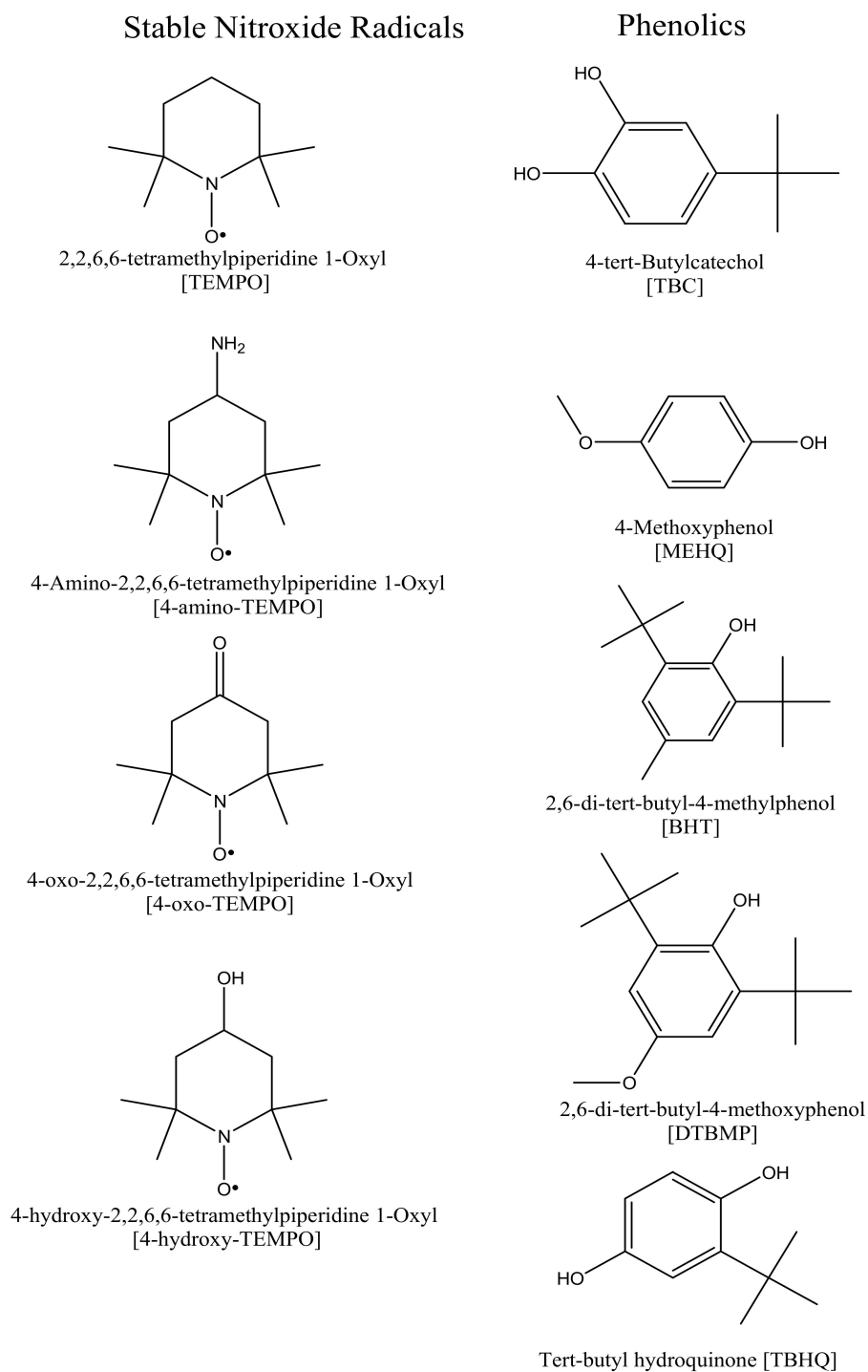


**Figure 4.** The name and structure of stable nitroxide radicals (SNR) and phenolic components. Hydrogen atoms are omitted for clarity.

The FT-IR spectra were recorded for UP seed (Figure 5). In the FT-IR spectrum of the UP seed, the peaks at  $3004\text{ cm}^{-1}$ – $3083\text{ cm}^{-1}$  are attributed to the  $\text{sp}^2$  C-H stretch, and band at  $2923\text{ cm}^{-1}$  and  $2850\text{ cm}^{-1}$  corresponds to the  $\text{sp}^3$  C-H stretch. Also, signals at  $1630\text{ cm}^{-1}$ – $1680\text{ cm}^{-1}$  are assigned to the stretching vibrations of aromatic C=C in the UP seed. The signal at  $1452\text{ cm}^{-1}$  corresponding to  $\text{CH}_2 + \text{C}=\text{C}$  bond stretching. Finally, a slight shift of C–O aromatic stretching modes towards lower wavenumbers can be observed.

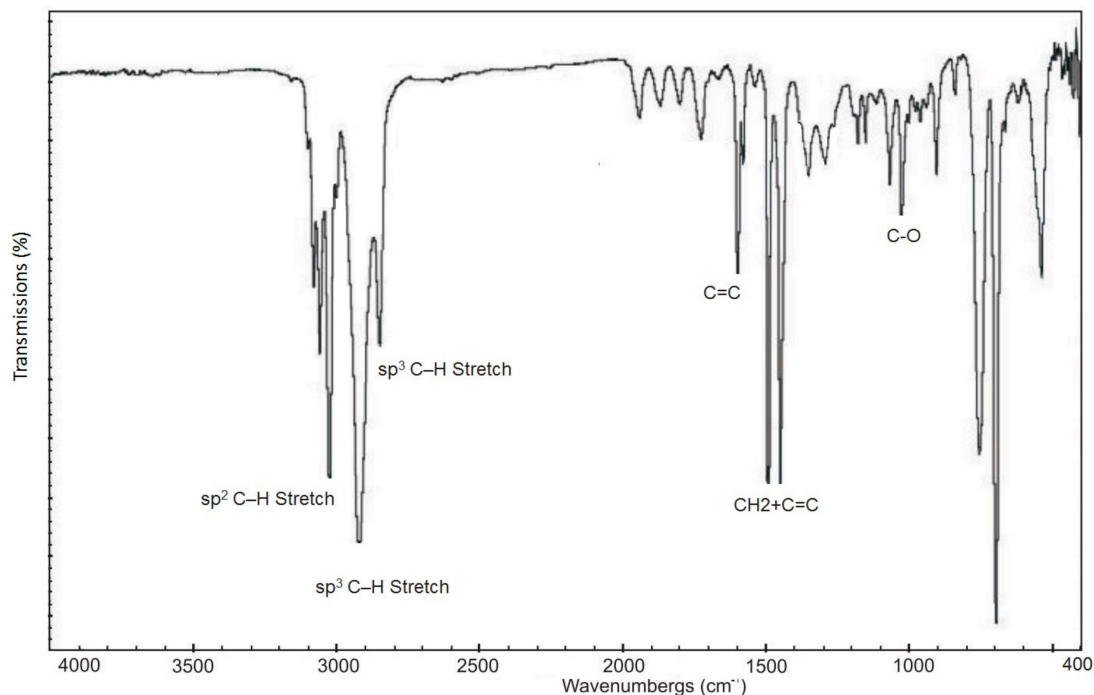


**Figure 5.** The FT-IR spectrum of undesired polymer seed.

### 2.2.2. Thermogravimetric Analysis

The initial decomposition temperature is measured via thermogravimetric analysis (TGA) test. The test is performed from ambient temperature up to 350 °C with 10 °C/min temperature ramp and under a nitrogen flow.

### 2.2.3. Analysis of Product (Styrene, Dimer Styrene, and Trimer Styrene)

The samples were analyzed by GC-MS (model: Agilent 7890A series GC coupled with an Agilent 5975C series MS detector), equipped with a HP-5MS capillary column (inner diameter: 250  $\mu\text{m}$ ; film thickness: 0.25  $\mu\text{m}$ ; length: 30 m).

### 2.2.4. FTIR

The structural changes of sample were characterized by an attenuated total reflection Fourier-transformed infrared spectroscopy (ATR/FT-IR).

### 2.2.5. Inhibition Test

The effect of SNRs, phenolic compounds, and their blends on the polymerization of ST at 115 °C was evaluated by utilizing the apparatus depicted in Figure 6. The system includes an adiabatic cell reactor (ACR), which is made of stainless steel (60 mm length, and 50 mm inside diameter). A K-type thermocouple installed in the middle of ACR is employed to control the ACR temperature. Syringe pumps supply the desired mass of monomer, inhibitor, and water. Before initiation, oxygen is eliminated by nitrogen purge to avoid peroxide formation. The ST polymer was utilized as the nucleation source. The sample was then placed in the ACR, 2 mL of deionized water as an oxygen source was injected into the system, and after adding a 50 ppm inhibitor, 50 mL of monomer was injected. The oxygen dissolved in water acts as initiator. The concentration of dissolved oxygen in water equaled 8.5 mg/L [47]. After 4 h of polymerization, the reacting mixture was cooled, and the polymer was precipitated by adding about 5 mL of methanol. The precipitate was filtered, dried at 100 °C to remove methanol, and weighed. The experimental conditions are tabulated in Table 1.



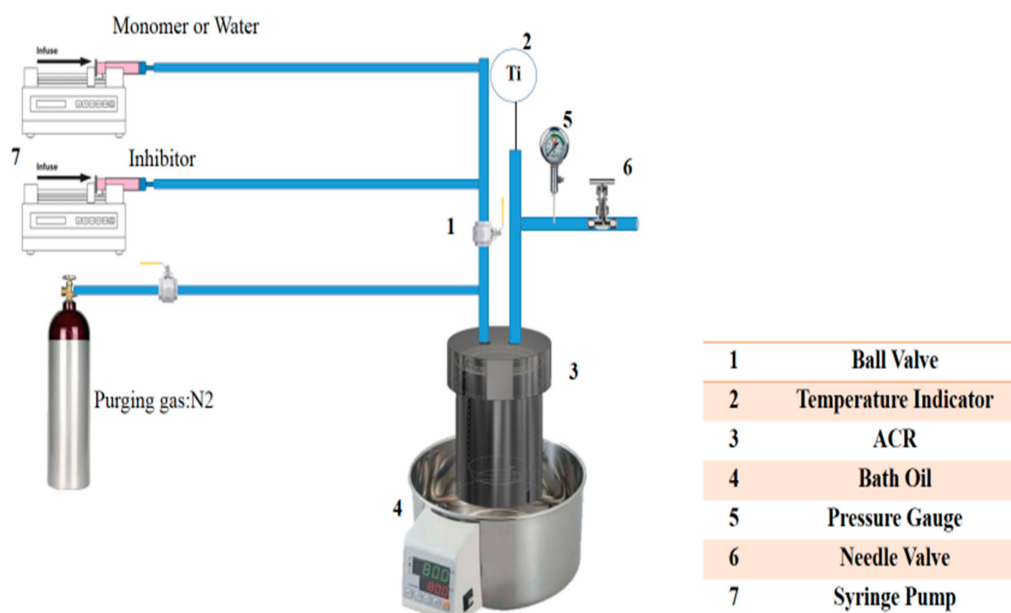


**Figure 6.** The schematic diagram of experimental setup.

**Table 1.** Experimental conditions.

Properties	Value	Unit
Temperature	115	°C
Pressure	1	bar
Inhibitor dosing	50	ppm
Monomer volume	50	mL
Water dosing	2	mL
Initial weight of ST polymer	0.2	g

### 3. Result

Different inhibitors and their blends were investigated to examine the effect of the inhibitor on the growth and formation of UP as well as ST conversion. As aforementioned, these studies are based on the DFT calculation and an experimental procedure.

#### 3.1. DFT Calculation Results

The results of DFT calculations applied on SNRs and phenolics are tabulated in Table 2.

**Table 2.** Calculated values of  $\mu$ ,  $\eta$ , and  $\omega$  indexes for SNRs and phenolics.

Sample ID	Component	$\mu$	$\eta$	$\omega$
<b>SNRs</b>				
S1	TEMPO	-3.1688	2.4450	2.0170
S2	4-amino-TEMPO	-3.4344	2.5718	2.2675
S3	4-oxo-TEMPO	-3.6544	2.1485	3.1079
S4	4-hydroxy-TEMPO	-3.8239	1.6973	4.3075
<b>Phenolics</b>				
S5	BHT	-2.6654	2.9900	1.1880
S6	TBC	-3.2072	2.7878	1.8448
S7	TBHQ	-3.2376	2.6937	1.9457
S8	DTBMP	-2.5161	2.8021	1.1297
S9	MEHQ	-3.2282	2.6478	1.9680

As mentioned previously, inhibitors are divided into antipolymers (i.e., S1, S2, S3, and S4 in Table 2) and antioxidants (S5, S6, S7, S8, and S9 in Table 2). The most important difference is that for the antipolymers, higher electrophilicity is desirable, while it is reverse for the antioxidants. In other words, for the purpose of inhibiting polymerization, a suitable antipolymer should possess higher electrophilicity, and inversely, a suitable antioxidant should have lower electrophilicity.

Among the first group (i.e., antipolymers), TEMPO has the lowest electrophilicity index, indicating that this antipolymer has the lowest reactivity, and thus it is more stable. Conversely, the highest electrophilicity index of 4-hydroxy TEMPO indicates that it is less stable and more reactive in comparison with other SNR inhibitors. In addition, it is known that the hardness index is related to molecular stability, and consequently higher hardness means higher stability of molecule [48,49]. In this respect, hard molecules (e.g., TEMPO and 4-amino-TEMPO) possess higher values of chemical hardness, and subsequently, larger gaps between the HOMO and LUMO, whereas soft molecules (e.g., 4-hydroxy-TEMPO and 4-oxo-TEMPO) exhibit lower values of chemical hardness and smaller gaps. The obtained results demonstrate good consistency with those reported in the previous studies [50].

To compare performance of the second group inhibitors (i.e., antioxidants), firstly it should be noted that the distribution of the HOMO energy is a criterion of inhibitory performance of phenolic antioxidants. Thus, considering the fact that the molecules with lower gap energy shows weaker electrophilicity [51,52], among the studied phenolics, DTBMP (1.1297 eV) and BHT (1.1880 eV) possess higher electrophilicity in comparison with TBC (1.8448 eV), TBHQ (1.9457 eV), and MEHQ (1.9680 eV).

The electrophilicity of selected SNRs and phenolics that are calculated utilizing DFT are presented in Figure 7.

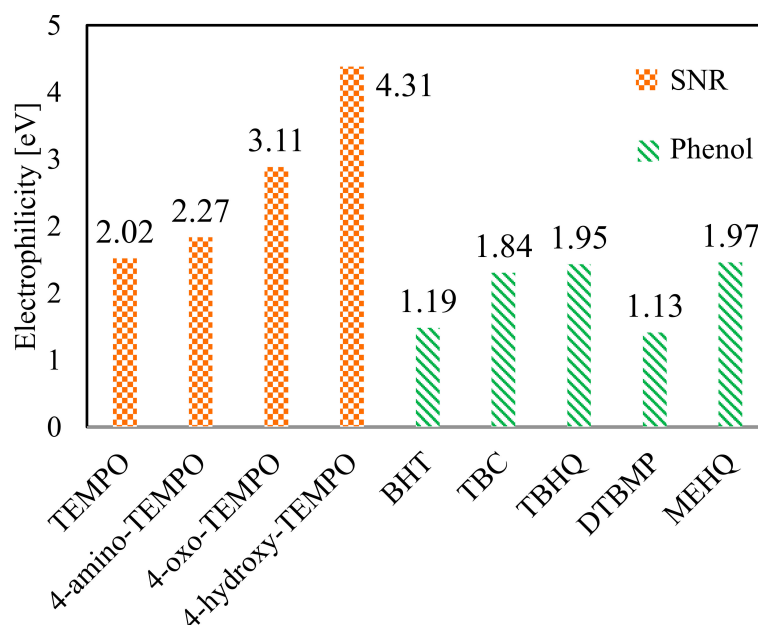


**Figure 7.** Calculated electrophilicity of SNRs and phenolics utilizing density functional theory (DFT).

For the case of antipolymers, based on the theoretical studies [53], the capability of hydrogen bonding by SNRs affects the properties and proton affinities. In fact, the present oxygen in the N–O bond of SNRs is a suitable H-bond acceptor. The mentioned oxygen can compete with other oxygen atoms, which are present within the structure, even in the solid state. It is observed that the order of electrophilicity of SNRs is: 4-hydroxy-TEMPO > 4-oxo-TEMPO > 4-amino-TEMPO > TEMPO. Hence, it is expected that 4-oxo-TEMPO shows the best inhibition effect in the UP formation and styrene conversion.

For the case of antioxidants, however, it can be observed that electrophilicity of phenolic antioxidants are in the following order: MEHQ > TBHQ > TBC > BHT > DTBMP. Hence, DTBMP is expected to show the best inhibition effect in the UP formation.

In order to acquire a deeper understanding of the performance of different inhibitors and to confirm the findings of DFT calculations, the experimental results are presented and compared in the following section.

### 3.2. Experimental Results

The growth percentage, which is calculated by Equation (4), is considered as a criterion to compare the performance of inhibitors.

$$\text{Growth \%} = \frac{\text{weight}_{\text{Final}} - \text{weight}_{\text{Initial}}}{\text{weight}_{\text{Initial}}} \times 100 \quad (4)$$

The initial weight equals to nucleation source, and the final weight equals to the summation of UP formation weight added to the initial weight. Firstly, it should be noted that aside from the UP formation, dimer and oligomer formation is inevitable as well. However, the number of undesired dimers and oligomers production is very small because the radical mechanism is prevailing, which mainly leads to the polymerization. However, these quantities must be controlled in a specified range because dimers and oligomers are regarded as impurities, which do not participate in further reactions in the polymerization unit. As a result, they must be separated in the styrene purification unit.

In this set of experiments, styrene conversion as well as the formation of dimers and oligomers are investigated after 4 and 8 h of operation to ensure those small quantities of dimer and oligomer are generated. In this respect, Tables 3 and 4 tabulate the effects of inhibitors on the weight and growth of undesired polymer, the quantities of generated dimer and oligomer, and conversion of styrene. The obtained results reveal that inhibition effects do not change significantly when the reaction time increases from 4 to 8 h, and they are approximately identical.

**Table 3.** Measured weights of polymer and the growth percentage in the presence of inhibitors after 4 h.

Sample ID	Component	Weight [g]	Growth Percentage	Outlet Mass Fraction [wt.%]			Conversion [%]
				SNRs	Styrene	Dimer	
S1	TEMPO	0.395	97.35	99.719	0.034	0.015	0.231
S2	4-amino-TEMPO	0.320	60.05	99.808	0.021	0.009	0.142
S3	4-oxo-TEMPO	0.313	56.30	99.811	0.020	0.009	0.134
S4	4-hydroxy-TEMPO	0.250	24.85	99.885	0.013	0.006	0.065
				Styrene	Dimer	Trimer	
S5	BHT	0.285	42.50	99.839	0.022	0.010	0.111
S6	Commercial TBC	0.305	52.65	99.811	0.028	0.012	0.139
S7	TBHQ	0.363	81.25	99.749	0.034	0.015	0.201
S8	DTBMP	0.233	16.40	99.902	0.012	0.005	0.048
S9	MEHQ	0.387	93.35	99.730	0.053	0.023	0.251

**Table 4.** Measured weights of polymer and the growth percentage in the presence of inhibitors after 8 h.

Sample ID	Component	Weight [g]	Growth Percentage	Outlet Mass Fraction [wt.%]			Conversion [%]
				SNRs	Styrene	Dimer	
S1	TEMPO	0.474	136.82	99.630	0.045	0.019	0.320
S2	4-amino-TEMPO	0.464	132.07	99.654	0.034	0.015	0.296
S3	4-oxo-TEMPO	0.422	111.00	99.703	0.035	0.015	0.257
S4	4-hydroxy-TEMPO	0.350	74.79	99.783	0.019	0.008	0.167
				Styrene	Dimer	Trimer	
S5	BHT	0.399	99.50	99.713	0.036	0.015	0.237
S6	Commercial TBC	0.470	135.08	99.643	0.038	0.016	0.307
S7	TBHQ	0.526	162.81	99.568	0.054	0.023	0.382
S8	DTBMP	0.319	59.47	99.812	0.019	0.008	0.138
S9	MEHQ	0.630	215.16	99.493	0.062	0.027	0.491

The obtained results regarding styrene conversion is proportionally in agreement with that of UP growth. Hence, only one of these two parameters is required to be evaluated as the inhibition criterion. It should also be mentioned that the styrene dimer and trimer only refer to 2,4-diphenyl-1-butene and 2,4,6-triphenyl-1-hexene, respectively.

The lower weight of polymer, growth percentage, and conversion all imply better inhibition effect. Hence, 4-hydroxy-TEMPO and DTBMP offer better inhibition effect among the SNRs and phenolics, respectively. It can be understood from the result that the substituent in the 4'-position of the cyclic structure has a significant effect on the ability of TEMPO in inhibiting polymerization. Consequently, among the SNRs, 4-hydroxy TEMPO (24.85% growth and 0.065% conversion) and 4-oxo-TEMPO (56.3% growth and 0.134% conversion) have the greatest effectiveness, respectively, after 4 h. As presented in Tables 3 and 4, the styrene conversion and polymerization inhibition performance of phenolics are in the following order: DTBMP > BHT > commercial TBC > TBHQ > MEHQ. Results show that DTBMP and BHT are the most effective phenolics.

The experimental results of growth percentage are plotted against the calculated electrophilicity from DFT calculations in Figure 8. The observed trends show that in SNRs, increase in electrophilicity leads to lower growth percentage, while in the phenolics, higher growth percentage can be seen with the increase in electrophilicity. Consequently, phenolics with lower electrophilicity and SNRs with higher electrophilicity are preferred. Such a difference could be explained by different mechanisms presented in Figure 1 (see r5, r6, and r9).

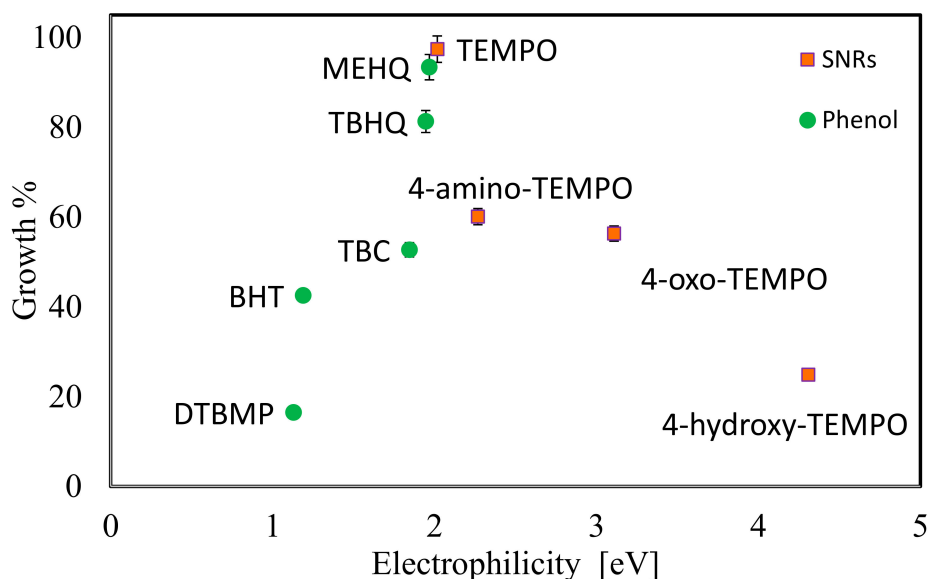


**Figure 8.** Calculated electrophilicity and measured growth percentage after 4 h of SNRs and phenolics.

A comparison of electrophilicity and growth percentage of 4-amino-TEMPO and 4-oxo-TMEPO reveals that in spite of the considerable difference in electrophilicity, their growth percentage differs slightly. This observation can be attributed to their different thermal behavior at various experimental condition. Actually, the key parameter that plays a very influential role in the performance of inhibitors is the operating temperature, which is around 115 °C in the styrene purification process. To clarify the thermal behavior of inhibitors toward temperature, TGA patterns, which determine the initial decomposition temperature, are shown in Figure 9a,b.

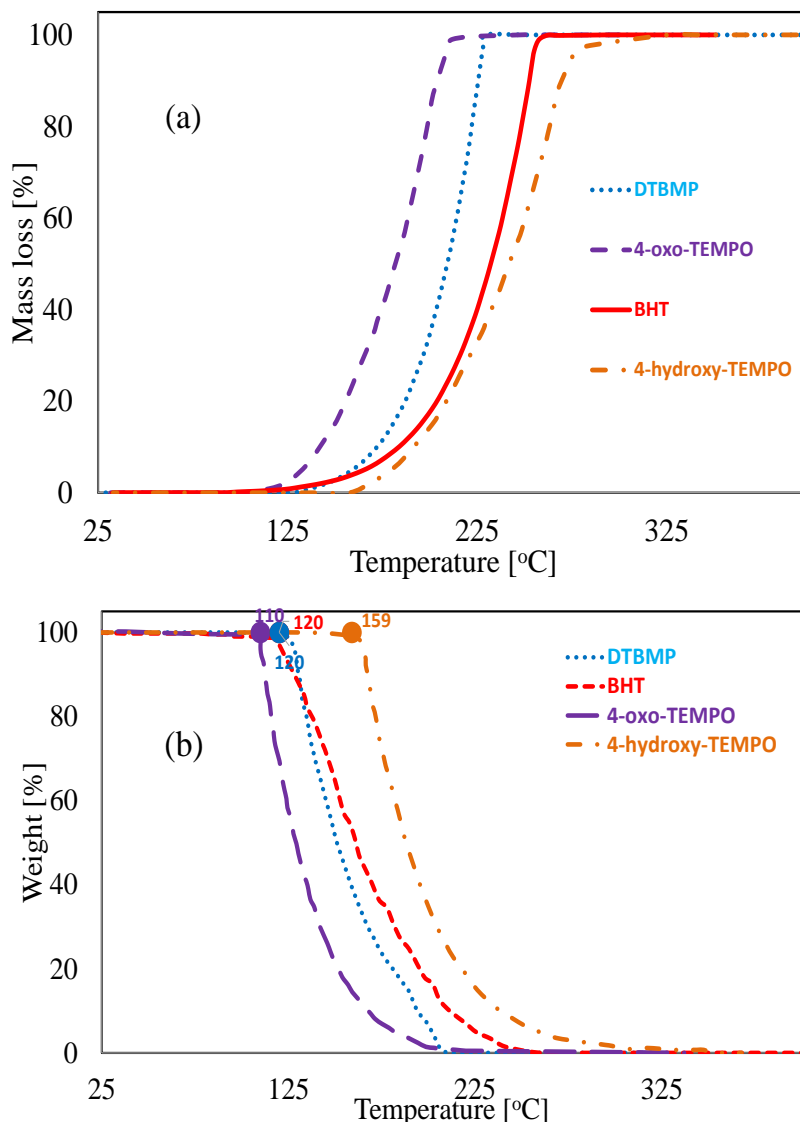


**Figure 9.** Thermogravimetric analysis of BHT, DTBMP, 4-hydroxy-TEMPO, and 4-oxo-TEMPO. (a) mass loss % and; (b) weight %.

In fact, as the temperature reaches the initial decomposition temperature, the inhibitors start to break down, and thereby lose their capability of inhibiting polymerization. As displayed in Figure 9, the initial decomposition temperature of BHT, DTBMP, and 4-hydroxy-TEMPO are higher than 115 °C, while that of 4-oxo-TEMPO starts from 110 °C. These results imply that at the operating temperature of 115 °C, 4-oxo-TEMPO molecules decompose and lose their ability in UP inhibition.

The mechanism of 4-oxo-TEMPO decomposition, which is called keto-enol tautomerism, is well-explained in the literature [54,55]. Through the decomposition of 4-oxo-TEMPO, nitroso and hydroxylamine compounds are formed, which is followed by further decomposition of nitroso and hydroxylamine compounds, leading to production of TEMPOH and TEMPO with low electrophilicity. The formation of less electrophilic TEMPOH and TEMPO justifies the unexpected performance of 4-oxo-TEMPO molecule, considering its high electrophilicity [54,55].

The functional groups of the 4-oxo-TEMPO and its decomposition products are further characterized by FT-IR to investigate the chemical structure changes during 4-oxo-TEMPO heating. The FT-IR spectra in the range of 400–4000  $\text{cm}^{-1}$  are shown in Figure 10. The peaks at 1700  $\text{cm}^{-1}$  in the FT-IR spectra of 4-oxo-TEMPO were assigned to the C=O stretching mode. For decomposition product of 4-oxo-TEMPO, no peak at 1700  $\text{cm}^{-1}$  (main peak for 4-oxo-TEMPO) is observed, which means the

breakage of C=O bond in 4-oxo-TEMPO, and absence of 4-oxo-TEMPO in the decomposition product. This finding provides another strong evidence which indicates that the mass losses observed in the TGA is merely attributed to the decomposition of 4-oxo-TEMPO, rather than other reasons (e.g., boiling or evaporation).

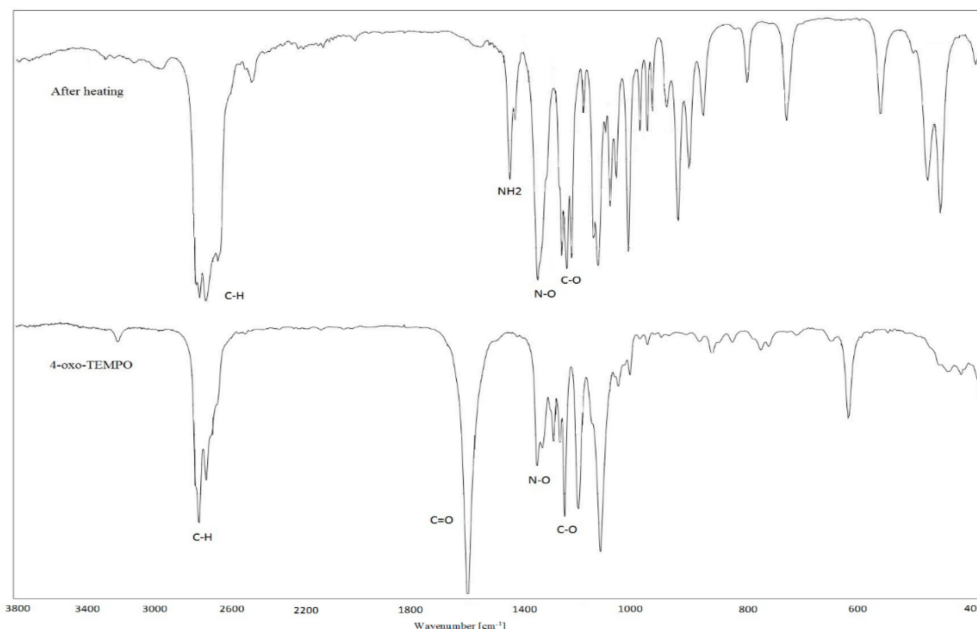


**Figure 10.** The FTIR spectrum of 4-oxo-TEMPO and decomposition products of 4-oxo-TEMPO.

As previously mentioned, 4-hydroxy-TEMPO and 4-oxo-TEMPO from SNRs and DTMBP and BHT from phenolics show the best performance in the inhibition of UP and styrene conversion. Hence, their synergistic effect in the inhibition process is worth investigating.

### 3.3. Synergistic effect of Antioxidant and Antipolymer

In order to determine the synergistic effect of the optimum blend of antioxidants and antipolymers in the inhibition process, a mixture of antioxidants and antipolymers (50 wt.%), which is injected to the process with the overall concentration of 50 ppm, was prepared and evaluated at the experimental conditions explained previously.

As tabulated in Table 5, the blends of optimum antioxidants and antipolymers improve the inhibition process in comparison with the commercial TBC sample. Moreover, the results show that the blends illustrate superior performance relative to single-component inhibitors, which arises from the fact that antipolymers are responsible for the inhibition of two polymerization pathways (i.e., r1–r3 and r7–r8 shown in Figure 1) and antioxidants just terminate the other polymerization pathway (i.e., r2–r6). The growth percentage of DTMBP/4-hydroxy-TEMPO, DTMBP/4-oxo-TEMPO, and BHT/4-hydroxy-TEMPO blends are 8.60, 10.25, and 12.65, respectively.

**Table 5.** Measured weights of polymer and the growth percentage in the presence of inhibitor blends after 4 h.

Sample ID	Component	Weight [g]	Growth Percentage
S6	Commercial TBC	0.3053	52.65
S10	DTMBP/4-hydroxy-TEMPO	0.2042	8.60
S11	DTMBP/4-oxo-TEMPO	0.2185	10.25
S12	BHT/4-hydroxy-TEMPO	0.2093	12.65
S13	BHT/4-oxo-TEMPO	0.2847	42.35

The growth percentage of all the single and blended inhibitors are compared in Figure 11. As can be seen, the inhibitor composed of DTMBP/4-hydroxy-TEMPO provides the best inhibition performance, while TEMPO shows the worst one.

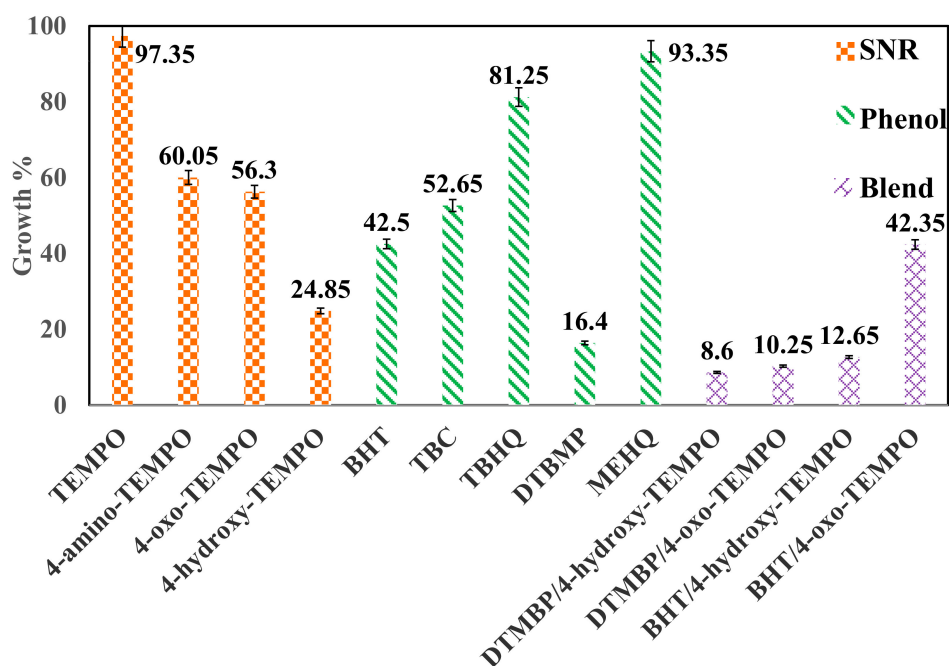


Figure 11. Growth percentage of SNRs, phenolics, and blends.

The synergism of SNRs and phenolics blends depends on the reversible hydrogen atom transfer between them. In fact, by utilizing the blends of SNRs and phenolics, hydrogen acceptance by SNRs and hydrogen donation by phenolics are enhanced, which is followed by improvement in inhibition performance.

Hydrogen atom hopping between 4-hydroxy-TEMPO and DTMBP results in a dynamic equilibrium of phenoxyl radical and 4-hydroxy-TEMPO. The phenoxyl radical can abstract the labile hydrogen from the product of dimerization of styrene Diels-Alder self-reaction [56,57]. This reaction yields a high flux of alkyl radicals and accelerates oxygen consumption. Hydrogen abstraction from DTMBP by TEMPO is not favorable due to the bond dissociation energies of TEMPOH and MEHQ [58]. The reaction is driven by hydrogen abstraction from styrene dimer by the phenoxyl radical to form an aromatic compound.

The blend of BHT/4-oxo-TEMPO did improve the inhibition of UP. This is, in fact, due to low abstraction of BHT hydrogen by the 4-oxo-TEMPO and decomposition of 4-oxo-TEMPO.

The effect of concentration of DTMBP/4-hydroxy-TEMPO blend on the inhibition process is depicted in Figure 12. The obtained results reveal that the blend of 4-hydroxy-TEMPO (25 wt.%) and DTMBP (75 wt.%), causes the lowest growth percentage, and thereby higher inhibition efficiency is obtained. However, other concentrations are also more effective than single SNR or phenolic compounds.

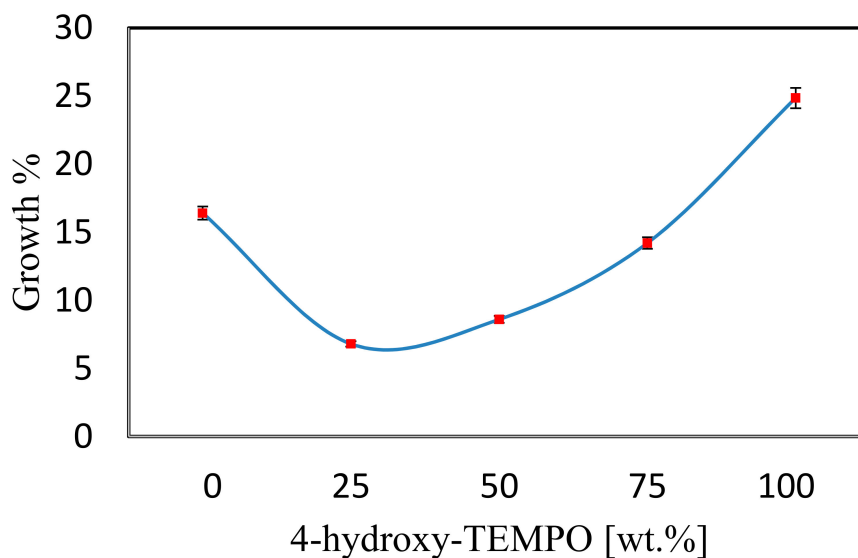


**Figure 12.** The effect of DTMBP/4-hydroxy-TEMPO concentration on the growth percentage.

#### 4. Conclusions

The DFT calculation and an experimental procedure were employed to analyze the inhibition performance of various antioxidants and antipolymer inhibitors regarding the undesired styrene polymerization during styrene purification process. The electrophilicity index and growth percentage (or styrene conversion) were obtained by DFT calculation and experiments, respectively. Furthermore, the relation between the calculated electrophilicity and the measured growth percentage and styrene conversion was determined. In addition, in order to find the optimum inhibitor, both growth percentage and electrophilicity were taken into consideration. Accordingly, 4-oxo-TEMP and 4-hydroxy-TEMPO were the best antipolymers, while DTMBP and BHT were the best antioxidant inhibitors. After four hours of operation, the lowest growth percentage of 16.40 and conversion percentage of 0.048 were obtained in the case of DTBMP. Besides, the synergistic effect of antioxidant and antipolymer inhibitors were also investigated by the experimental procedure. Results showed that a combination of 4-hydroxy-TEMPO (25 wt.%) and DTMBP (75 wt.%) provided the best synergistic inhibition effect with the lowest growth percentage of 8.60 after 4 h of operation.

**Author Contributions:** A.D.: Conceived and designed the analysis, Collected the data, Contributed data or analysis tools, Performed the analysis, Wrote the paper; M.R.R.: Conceived and designed the analysis, Contributed data or analysis tools, Performed the analysis, Wrote the paper; S.R.: Conceived and designed the analysis, Performed the analysis, Wrote the paper.

**Funding:** This research received no external funding.

**Conflicts of Interest:** The authors confirm that there are no known conflict of interest associated with this publication and there has been no significant financial support for this work that could have influenced its outcome.

#### References

1. Cai, S.; Zhang, B.; Cremaschi, L. Review of moisture behavior and thermal performance of polystyrene insulation in building applications. *Build. Environ.* **2017**, *123*, 50–65. [[CrossRef](#)]
2. Ghosh, J.; Ghorai, S.; Bhunia, S.; Roy, M.; De, D. The role of devulcanizing agent for mechanochemical devulcanization of styrene butadiene rubber vulcanizate. *Polym. Eng. Sci.* **2018**, *58*, 74–85. [[CrossRef](#)]
3. Kamelian, F.S.; Saljoughi, E.; Nasirabadi, P.S.; Mousavi, S.M. Modifications and research potentials of acrylonitrile/butadiene/styrene (ABS) membranes: A review. *Polym. Compos.* **2018**, *39*, 2835–2846. [[CrossRef](#)]
4. Dimian, A.C.; Bildea, C.S. Energy Efficient Styrene Process: Design and Plantwide Control. *Ind. Eng. Chem. Res.* **2019**, *58*, 4890–4905. [[CrossRef](#)]



5. Ovejero, G.; Romero, M.D.; Díaz, I.; Mestanza, M.; Díez, E. Bentonite as an Alternative Adsorbent for the Purification of Styrene Monomer: Adsorption Kinetics, Equilibrium and Process Design. *Adsorpt. Sci. Technol.* **2010**, *28*, 101–123. [[CrossRef](#)]
6. Díaz, I.; Langston, P.; Ovejero, G.; Romero, M.D.; Díez, E. Purification process design in the production of styrene monomer. *Chem. Eng. Process Process Intensif.* **2010**, *49*, 367–375. [[CrossRef](#)]
7. Miller, G.H.; Perizzolo, A.F. Styrene popcorn polymers. *J. Polym. Sci.* **1955**, *18*, 411–416. [[CrossRef](#)]
8. Hsieh, H.; Quirk, R.P. *Anionic Polymerization: Principles and Practical Applications*; CRC Press: Boca Raton, FL, USA, 1996.
9. Liao, C.-C.; Wu, S.-H.; Su, T.-S.; Shyu, M.-L.; Shu, C.-M. Thermokinetics evaluation and simulations for the polymerization of styrene in the presence of various inhibitor concentrations. *J. Therm. Anal. Calorim.* **2006**, *85*, 65–71. [[CrossRef](#)]
10. Chen, C.-C.; Duh, Y.-S.; Shu, C.-M. Thermal polymerization of uninhibited styrene investigated by using microcalorimetry. *J. Hazard. Mater.* **2009**, *163*, 1385–1390. [[CrossRef](#)]
11. Nanda, A.; Kishore, K. Autocatalytic oxidative polymerization of indene by cobalt porphyrin complex and kinetic investigation of the polymerization of styrene. *Macromolecules* **2001**, *34*, 1600–1605. [[CrossRef](#)]
12. Cui, J.; Ni, L.; Jiang, J.; Pan, Y.; Wu, H.; Chen, Q. Computational Fluid Dynamics Simulation of Thermal Runaway Reaction of Styrene Polymerization. *Org. Process Res. Dev.* **2019**, *23*, 389–396. [[CrossRef](#)]
13. Mohammadi, Y.; Pakdel, A.S.; Saeb, M.R.; Boodhoo, K. Monte Carlo simulation of free radical polymerization of styrene in a spinning disc reactor. *Chem. Eng. J.* **2014**, *247*, 231–240. [[CrossRef](#)]
14. Sobani, M.; Haddadi-Asl, V.; Mirshafiei-Langari, S.-A.; Salami-Kalajahi, M.; Roghani-Mamaqani, H.; Khezri, K. A kinetics study on the in situ reversible addition–fragmentation chain transfer and free radical polymerization of styrene in presence of silica aerogel nanoporous particles. *Des. Monomers Polym.* **2014**, *17*, 245–254. [[CrossRef](#)]
15. Sütekin, S.D.; Atıcı, A.B.; Güven, O.; Hoffman, A.S. Controlling of free radical copolymerization of styrene and maleic anhydride via RAFT process for the preparation of acetaminophen drug conjugates. *Radiat. Phys. Chem.* **2018**, *148*, 5–12. [[CrossRef](#)]
16. Matyjaszewski, K.; Davis, T.P. *Handbook of Radical Polymerization*; John Wiley & Sons: Hoboken, NJ, USA, 2003.
17. Chiefari, J.; Chong, Y.; Ercole, F.; Krstina, J.; Jeffery, J.; Le, T.P.; Mayadunne, R.T.A.; Meijs, G.F.; Moad, C.L.; Moad, G. Living free-radical polymerization by reversible addition—Fragmentation chain transfer: the RAFT process. *Macromolecules* **1998**, *31*, 5559–5562. [[CrossRef](#)]
18. Encinas, M.V.; Lissi, E.A.; Norambuena, E. Inhibition of Styrene Polymerization by  $\beta$ -Nitrostyrene. A Novel Inhibition Mechanism. *Macromolecules* **1998**, *31*, 5171–5174. [[CrossRef](#)]
19. Harper, C.A.; Petrie, E.M. *Plastics Materials and Processes: A Concise Encyclopedia*; John Wiley & Sons: Hoboken, NJ, USA, 2003.
20. Luo, K.; Zheng, W.; Zhao, X.; Wang, X.; Wu, S. Effects of antioxidant functionalized silica on reinforcement and anti-aging for solution-polymerized styrene butadiene rubber: Experimental and molecular simulation study. *Mater. Des.* **2018**, *154*, 312–325. [[CrossRef](#)]
21. Gomes, G.d.P.; Loginova, Y.; Vatsadze, S.Z.; Alabugin, I.V. Isonitriles as Stereoelectronic Chameleons: The Donor–Acceptor Dichotomy in Radical Additions. *J. Am. Chem. Soc.* **2018**, *140*, 14272–14288. [[CrossRef](#)]
22. Kolthoff, I.; Bovey, F. Studies of Retarders and Inhibitors in the Emulsion Polymerization of Styrene. I. Retarders1a. *J. Am. Chem. Soc.* **1948**, *70*, 791–799. [[CrossRef](#)]
23. Bevington, J.; Ebdon, J.; Huckerby, T. An appraisal of NMR methods for study of end-groups derived from initiators in radical polymerizations. *Eur. Polym. J.* **1985**, *21*, 685–694. [[CrossRef](#)]
24. Yokota, H.; Kawakatsu, T. Modeling induction period of polymer crystallization. *Polymer* **2017**, *129*, 189–200. [[CrossRef](#)]
25. Cohen, S.G. Inhibition and Retardation of the Peroxide Initiated Polymerization of Styrene. *J. Am. Chem. Soc.* **1947**, *69*, 1057–1064. [[CrossRef](#)]
26. Wright, J.S.; Carpenter, D.J.; McKay, D.J.; Ingold, K. Theoretical calculation of substituent effects on the O–H bond strength of phenolic antioxidants related to vitamin E. *J. Am. Chem. Soc.* **1997**, *119*, 4245–4252. [[CrossRef](#)]
27. Wright, J.S.; Johnson, E.R.; DiLabio, G.A. Predicting the activity of phenolic antioxidants: Theoretical method, analysis of substituent effects, and application to major families of antioxidants. *J. Am. Chem. Soc.* **2001**, *123*, 1173–1183. [[CrossRef](#)] [[PubMed](#)]

28. Tikhonov, I.; Roginsky, V.; Pliss, E. The chain-breaking antioxidant activity of phenolic compounds with different numbers of O-H groups as determined during the oxidation of styrene. *Int. J. Chem. Kinet.* **2009**, *41*, 92–100. [[CrossRef](#)]
29. Mardare, D.; Matyjaszewski, K. *Thermal Polymerization of Styrene in the Presence of Stable Radicals and Inhibitors*; Carnegie-Mellon Univ. Pittsburgh Pa. Dept of Chemistry: Pittsburgh, PA, USA, 1994.
30. Kemmere, M.; Mayer, M.; Meuldijk, J.; Drinkenburg, A. The influence of 4-tert-butylcatechol on the emulsion polymerization of styrene. *J. Appl. Polym. Sci.* **1999**, *71*, 2419–2422. [[CrossRef](#)]
31. Finson, S.; Jury, J.M.; Crivello, J.V. Azodioxides as Inhibitors and Retarders in Photoinitiated Cationic Polymerization. *Macromol. Chem. Phys.* **2013**, *214*, 1806–1816. [[CrossRef](#)]
32. Moghadam, N.; Liu, S.; Srinivasan, S.; Grady, M.C.; Soroush, M.; Rappe, A.M. Computational Study of Chain Transfer to Monomer Reactions in High-Temperature Polymerization of Alkyl Acrylates. *J. Phys. Chem. A* **2013**, *117*, 2605–2618. [[CrossRef](#)]
33. Bartlett, P.D.; Kwart, H. Some Inhibitors and Retarders in the Polymerization of Liquid Vinyl Acetate. II. 1, 3, 5-Trinitrobenzene and Sulfur1. *J. Am. Chem. Soc.* **1952**, *74*, 3969–3973. [[CrossRef](#)]
34. Anbazhakan, K.; Sadasivam, K.; Praveena, R.; Dhandapani, M. Target prediction and antioxidant analysis on isoflavones of demethyltaxasin: A DFT study. *J. Mol. Model.* **2019**, *25*, 169. [[CrossRef](#)]
35. Sharma, V.; Arora, E.K.; Cardoza, S. 4-Hydroxy-benzoic acid (4-diethylamino-2-hydroxy-benzylidene) hydrazide: DFT, antioxidant, spectroscopic and molecular docking studies with BSA. *Luminescence* **2016**, *31*, 738–745. [[CrossRef](#)] [[PubMed](#)]
36. Tüdös, F.; Kende, I.; Azori, M. Inhibition kinetics of the polymerization of styrene. II. Investigations on the effect of s-trinitrobenzene. *J. Polym. Sci. Part A Gen. Pap.* **1963**, *1*, 1353–1368.
37. Tüdös, F.; Kende, I.; Azori, M. Inhibition kinetics of polymerization of styrene. III. Investigations on the effect of substituted trinitrobenzenes. *J. Polym. Sci. Part A Gen. Pap.* **1963**, *1*, 1369–1381.
38. Pellecchia, C.; Grassi, A. Syndiotactic-specific polymerization of styrene: Catalyst structure and polymerization mechanism. *Top. Catal.* **1999**, *7*, 125–132. [[CrossRef](#)]
39. Domingo, L.R.; Pérez, P. Global and local reactivity indices for electrophilic/nucleophilic free radicals. *Org. Biomol. Chem.* **2013**, *11*, 4350–4358. [[CrossRef](#)] [[PubMed](#)]
40. De Vleeschouwer, F.; van Speybroeck, V.; Waroquier, M.; Geerlings, P.; de Proft, F. Electrophilicity and nucleophilicity index for radicals. *Org. Lett.* **2007**, *9*, 2721–2724. [[CrossRef](#)] [[PubMed](#)]
41. Zheng, Y.-Z.; Zhou, Y.; Liang, Q.; Chen, D.-F.; Guo, R.; Xiong, C.-L.; Xu, X.J.; Zhang, Z.N.; Huang, Z.J.; Xu, X.J.; et al. Solvent effects on the intramolecular hydrogen-bond and anti-oxidative properties of apigenin: A DFT approach. *Dyes Pigments* **2017**, *141*, 179–187. [[CrossRef](#)]
42. Zheng, Y.-Z.; Chen, D.-F.; Deng, G.; Guo, R.; Fu, Z.-M. The antioxidative activity of piceatannol and its different derivatives: Antioxidative mechanism analysis. *Phytochemistry* **2018**, *156*, 184–192. [[CrossRef](#)]
43. Zheng, Y.-Z.; Chen, D.-F.; Deng, G.; Guo, R. The Substituent Effect on the Radical Scavenging Activity of Apigenin. *Molecules* **2018**, *23*, 1989. [[CrossRef](#)] [[PubMed](#)]
44. Zheng, Y.-Z.; Deng, G.; Chen, D.-F.; Liang, Q.; Guo, R.; Fu, Z.-M. Theoretical studies on the antioxidant activity of pinobanksin and its ester derivatives: Effects of the chain length and solvent. *Food Chem.* **2018**, *240*, 323–329. [[CrossRef](#)]
45. Wang, X.; Lin, F.; Qu, J.; Hou, Z.; Luo, Y. DFT Studies on Styrene Polymerization Catalyzed by Cationic Rare-Earth-Metal Complexes: Origin of Ligand-Dependent Activities. *Organometallics* **2016**, *35*, 3205–3214. [[CrossRef](#)]
46. Coote, M.L.; Henry, D.J. Computer-Aided Design of a Destabilized RAFT Adduct Radical: Toward Improved RAFT Agents for Styrene-block-Vinyl Acetate Copolymers. *Macromolecules* **2005**, *38*, 5774–5779. [[CrossRef](#)]
47. Kauffman, G. The Cost of Clean Water in the Delaware River Basin (USA). *Water* **2018**, *10*, 95. [[CrossRef](#)]
48. Cinar, Z. The role of molecular modeling in TiO<sub>2</sub> photocatalysis. *Molecules* **2017**, *22*, 556. [[CrossRef](#)] [[PubMed](#)]
49. Del Castillo, R.M.; Salcedo, R.; Martínez, A.; Ramos, E.; Sansores, L.E. Electronic Peculiarities of a Self-Assembled M12L24 Nanoball (M = Pd+ 2, Cr, or Mo). *Molecules* **2019**, *24*, 771. [[CrossRef](#)] [[PubMed](#)]
50. Galván, J.E.; Gil, D.M.; Lanús, H.E.; Altabef, A.B. Theoretical study on the molecular structure and vibrational properties, NBO and HOMO–LUMO analysis of the POX3 (X = F, Cl, Br, I) series of molecules. *J. Mol. Struct.* **2015**, *1081*, 536–542. [[CrossRef](#)]

51. Al-Majedy, Y.; Al-Duhaidahawi, D.; Al-Azawi, K.; Al-Amiery, A.; Kadhum, A.; Mohamad, A. Coumarins as potential antioxidant agents complemented with suggested mechanisms and approved by molecular modeling studies. *Molecules* **2016**, *21*, 135. [[CrossRef](#)]
52. Rao, P.S.; Puyad, A.L.; Bhosale, S.V.; Bhosale, S.V. Triphenylamine-Merocyanine-Based D1-A1- $\pi$ -A2/A3-D2 Chromophore System: Synthesis, Optoelectronic, and Theoretical Studies. *Int. J. Mol. Sci.* **2019**, *20*, 1621.
53. Ichikawa, K.; Sasada, R.; Chiba, K.; Gotoh, H. Effect of Side Chain Functional Groups on the DPPH Radical Scavenging Activity of Bisabolane-Type Phenols. *Antioxidants* **2019**, *8*, 65. [[CrossRef](#)]
54. Murayama, K.; Yoshioka, T. Studies on stable free radicals. IV. Decomposition of stable Nitroxide radicals. *Bull. Chem. Soc. Jpn.* **1969**, *42*, 2307–2309. [[CrossRef](#)]
55. Ma, Y.; Loyns, C.; Price, P.; Chechik, V. Thermal decay of TEMPO in acidic media via an N-oxoammonium salt intermediate. *Org. Biomol. Chem.* **2011**, *9*, 5573–5578. [[CrossRef](#)] [[PubMed](#)]
56. Boutevin, B.; Bertin, D. Controlled free radical polymerization of styrene in the presence of nitroxide radicals I. Thermal initiation. *Eur. Polym. J.* **1999**, *35*, 815–825. [[CrossRef](#)]
57. Conte, M.; Ma, Y.; Loyns, C.; Price, P.; Rippon, D.; Chechik, V. Mechanistic insight into TEMPO-inhibited polymerisation: Simultaneous determination of oxygen and inhibitor concentrations by EPR. *Org. Biomol. Chem.* **2009**, *7*, 2685–2687. [[CrossRef](#)] [[PubMed](#)]
58. Ma, Y. Nitroxides in Mechanistic Studies: Ageing of Gold Nanoparticles and Nitroxide Transformation in Acids. Ph.D. Thesis, University of York, York, UK, 2010.



© 2019 by the authors. Licensee MDPI, Basel, Switzerland. This article is an open access article distributed under the terms and conditions of the Creative Commons Attribution (CC BY) license (<http://creativecommons.org/licenses/by/4.0/>).